

Lattice QCD Constraints on Hybrid and Quark Stars

Yu.B. Ivanov,^{1, 2, *} A.S. Khvorostukhin,^{3, †} E.E. Kolomeitsev,^{4, ‡}
V.V. Skokov,^{1, 3, §} V.D. Toneev,^{1, 3, ¶} and D.N. Voskresensky^{1, 5, **}

¹*Gesellschaft für Schwerionenforschung mbH, Planckstr. 1, D-64291 Darmstadt, Germany*

²*Kurchatov Institute, Kurchatov sq. 1, Moscow 123182, Russia*

³*Joint Institute for Nuclear Research, RU-141980 Dubna, Moscow Region, Russia*

⁴*School of Physics and Astronomy, University of Minnesota, Minneapolis, MN 55455, USA*

⁵*Moscow Institute for Physics and Engineering, Kashirskoe sh. 31, RU-115409 Moscow, Russia*

(Dated: February 19, 2019)

A QCD-motivated dynamical-quasiparticle model with parameters adjusted to reproduce the lattice-QCD equation of state is extrapolated from region of high temperatures and moderate baryonic densities to the domain of high baryonic densities and zero temperature. The resulting equation of state matched with realistic hadronic equations of state predicts a phase transition into the quark phase at higher densities than those reachable in neutron star interiors. This excludes the possibility of the existence of hybrid (hadron-quark) stars. Pure quark stars are possible and have low masses, small radii and very high central densities. Similar results are obtained for a simple bag model with massive quarks, fitted to reproduce the same lattice results. Self-bound quark matter is also excluded within these models. Uncertainties in the present extrapolation are discussed. Comparison with standard bag models is made.

PACS numbers: 26.60.+c, 12.38.Mh, 12.39.Hg

Keywords: neutron star, lattice QCD

I. INTRODUCTION

Nowadays it is commonly accepted that the quark-gluon phase of the matter can be formed in the course of heavy-ion collisions at ultrarelativistic energies. There are indirect signatures that this state has been produced at Relativistic Heavy-Ion Collider (RHIC) [1]. On the other hand, it was suggested long ago [2] that quark matter may exist either in the interior of some stars or as a new family of pure quark stars. Then it was realized that some rather massive neutron stars may have a quark core (so called hybrid stars), cf. Ref. [3] and references therein. Recently the idea of quark pairing with high values of the gap (up to $\Delta \sim 100$ MeV) attracted much attention, cf. Ref. [4]. Observable signals of quark matter, presumably existing in interiors of hybrid and pure quark stars, are under extensive discussion. The most promising of these signals seem to be an abnormal mass-radius relation [5], r -mode spin-down [6], and a specific stellar cooling properties [7].

Although there is no *a priori* obstacle to existence of the quark matter in above the mentioned forms, the actual theoretical predictions are very uncertain. They hinge on the lack of understanding of the confinement mechanism in QCD. Therefore, parameters of theoretical quark models cannot be anchored to experimental

observables. Most of the treatments are based on either the standard or slightly modified MIT bag model, or the Nambu–Jona-Lasino (NJL) model, cf. Ref. [8] and references therein. In terms of a bag model, the main uncertainty is associated with the value of the vacuum pressure, i.e. the bag constant B_{eff} . The stellar properties are sensitive to this. A large value of B_{eff} excludes the existence of hybrid stars. With a decrease of B_{eff} , first the most massive neutron stars acquire a quark core, becoming hybrid stars. For a small B_{eff} , strange quark matter becomes absolutely stable, i.e. more stable than ^{56}Fe [9, 10]. Then pure quark stars (strangelets) of an arbitrary size may exist, being held together by strong rather than gravitational forces.

A straightforward calculation of the properties of strongly interacting matter and, in particular its equation of state (EoS), is possible on the lattice [11]. This technique is progressing rapidly. So far, the main body of lattice results concern the case of zero baryon chemical potential ($\mu = 0$) and finite temperatures. This case is just opposite to that of cold baryon matter present in the quark stars. Recently new lattice predictions on the EoS at finite, but small, baryon chemical potentials became available [12, 13, 14]. Nevertheless, they are still far from the astrophysically relevant domain. Therefore, a theoretical modeling is needed for their extrapolation.

The interpretation of these lattice results within phenomenological quasiparticle models, i.e. in terms of effectively massive quarks and gluons with a simple interaction, turned out to be very successful both at zero chemical potential [15, 16, 17, 18, 19, 20, 21, 22, 23, 24, 25, 26] and at small finite ones [23, 24, 25, 26]. With few phenomenological parameters it was possible to reasonably reproduce all lattice thermodynamic quantities. Effec-

*e-mail: Y.Ivanov@gsi.de

†e-mail: hvorost@thsun1.jinr.ru

‡e-mail: kolomeitsev@physics.umn.edu

§e-mail: V.Skokov@gsi.de

¶e-mail: V.Toneev@gsi.de

**e-mail: D.Voskresensky@gsi.de

tively the results can be interpreted in terms of a modified MIT bag model for massive quarks with density and temperature dependent bag constant and masses. These models can be used to extrapolate the lattice EoS to the domain of cold baryon matter. This has been done by Peshier, Kämpfer and Soff [19] for the thermodynamic quasiparticle model of Ref. [18]. They considered the possibility of the existence of quark stars and found a mass-radius relation for them. They concluded that quark stars with a mass larger than $1M_\odot$ may only exist for values of the effective bag constant $B^{1/4} \leq 180 - 200$ MeV, whereas their model produced a higher value. The possible existence of hybrid stars was not considered in that work. It is important to mention that the quasiparticle model of Ref. [19] was fitted only to the $\mu = 0$ lattice data available at that time and then it was extrapolated to finite values of the baryon chemical potential. The later fit of the same model to recent lattice data at finite baryon chemical potentials [12] resulted in somewhat different parameters of this quasiparticle model [23].

In this paper we would like to make “lattice QCD motivated” predictions on the possible existence of hybrid and quark stars, as well as their properties. To do this, we extrapolate the existing lattice results to the region of cold electroneutral baryon matter relying on the phenomenological QCD motivated dynamical-quasiparticle (DQ) model recently proposed in Ref. [26]. In equilibrium, at high temperatures the DQ model complies with the quasiparticle picture of the hard thermal loop approach [27], whereas at lower temperatures it simulates the confinement of the QCD. The latter is manifested by the fact that the solution to the model equations simply does not exist below certain combination of the temperature and the chemical potential. Two sets of parameters of this model (below denoted as “1-loop” and “2-loop”) were fitted to reproduce lattice data at finite baryon chemical potentials [12]. Extrapolation of the lattice data to the case of the cold baryon matter is essentially simpler in this model than in that of Ref. [19], where an implicit thermodynamic-consistency equation should be numerically solved. In fact, this advantage follows from an explicitly thermodynamically consistent formulation in terms of dynamic rather than thermodynamic variables.

In Sect. II we start with brief recapitulation of the DQ model. To have a reference point for the DQ model, we also consider three versions of the MIT bag model. Two “light-bag” models (“light-bag-155” and “light-bag-200”) with conventional current quark masses ($m_{u0} = 5$ MeV, $m_{d0} = 7$ MeV and $m_{s0} = 150$ MeV), zero gluon mass ($m_g = 0$) and different bag constants ($B^{1/4} = 155$ MeV and 200 MeV) covering a broad range of EoS’s usually applied to the treatment of hybrid and quark stars [28, 29]. We also consider a “heavy-bag” model, the quark/gluon masses and bag constant of which are fitted to reasonably reproduce the lattice results of Ref. [12]: $m_u = m_d = 330$ MeV, $m_s = 450$ MeV, $m_g = 600$ MeV and $B^{1/4} = 183$ MeV. In Sect. III we confront the predictions

of all these models to the (2+1)-flavor lattice data [12] at finite chemical potentials. In Sect. IV we derive the predictions of all the above models regarding the possible existence of hybrid and quark stars and discuss their properties.

II. MODELS

A. Dynamical-Quasiparticle Model

The effective Lagrangian of the DQ model [26] treats transverse gluons ϕ_a and quarks ψ_{fc} of $N_f = 3$ flavors and $N_c = 3$ colors. For this model it is essential that $N_f = N_c$. These constituents interact via mean fields $\zeta = \{\zeta_u, \zeta_d, \zeta_s\}$:

$$\mathcal{L} = \frac{1}{2} \sum_{a=1}^{N_g} [(\partial_\mu \phi_a)^2 - m_g^2(\zeta) \phi_a^2] + \sum_{c=1}^{N_c} \sum_{f=1}^{N_f} \bar{\psi}_{fc} [i\gamma_\mu \partial^\mu - m_f(\zeta)] \psi_{fc} - B(\chi), \quad (1)$$

where $N_g = 2(N_c^2 - 1)$ is the number of transverse gluons,

$$\chi^4 = \sum_{f=1}^{N_f} \zeta_f^4, \quad (2)$$

$$m_g^2 = \frac{2}{N_g} \sum_{f=1}^{N_f} \zeta_f^2 g^2(\chi), \quad (3)$$

$$m_f^2 - m_{f0}^2 = \frac{1}{2N_c} \zeta_f^2 g^2(\chi). \quad (4)$$

Here m_{f0} is the current f -quark mass, whereas m_g and m_f are effective masses of gluons (g) and quarks of flavor f , respectively. The masses and the coupling constant $g^2(\chi)$ depend on mean fields ζ .

$$B(\chi) = B_C - \frac{1}{N_g} [\chi^4 g^2(\chi) - \chi_C^4 g^2(\chi_C)] + \frac{2}{N_g} \int_{\chi_C}^\chi d\chi_1 \chi_1^3 g^2(\chi_1), \quad (5)$$

is the potential of the mean-field self-interaction having a meaning of an effective bag parameter. Here B_C and χ_C are parameters of the model.

The equations of motion for the mean fields read

$$-\frac{\partial \mathcal{L}}{\partial \zeta_i^2} = \frac{\partial B}{\partial \zeta_i^2} + \frac{1}{2} \frac{\partial m_g^2}{\partial \zeta_i^2} \eta^2 + \frac{1}{2} \sum_{f=1}^{N_f} \frac{\partial m_f^2}{\partial \zeta_i^2} \xi_f^2 = 0, \quad (6)$$

where

$$\eta^2 \equiv \sum_{a=1}^{N_g} \langle \phi_a^2 \rangle = \frac{N_g}{2\pi^2} \int_0^\infty \frac{k^2 dk}{(k^2 + m_g^2)^{1/2}} f_g(k), \quad (7)$$

$$\begin{aligned}\xi_f^2 &\equiv \sum_{c=1}^{N_c} \frac{\langle \bar{\psi}_{fc} \psi_{fc} \rangle}{m_f} \\ &= \frac{N_c}{\pi^2} \int_0^\infty \frac{k^2 dk}{(k^2 + m_f^2)^{1/2}} [f_{q,f}(k) + \bar{f}_{q,f}(k)],\end{aligned}\quad (8)$$

are scalar densities of gluons and quarks (divided by the mass), respectively, and $f_g(k)$, $f_{q,f}(k)$ and $\bar{f}_{q,f}(k)$ are occupation numbers (distribution functions) of gluons, quarks and antiquarks. In the case of equilibrium that we consider here, these are

$$f_g(k) = \frac{1}{\exp[(k^2 + m_g^2)^{1/2}/T] - 1}, \quad (9)$$

$$f_{q,f}(k) = \frac{1}{\exp\{[(k^2 + m_f^2)^{1/2} - \mu_f]/T\} + 1}, \quad (10)$$

$$\bar{f}_{q,f}(k) = \frac{1}{\exp\{[(k^2 + m_f^2)^{1/2} + \mu_f]/T\} + 1}, \quad (11)$$

where T is the temperature, and μ_f is the f -flavor quark chemical potential. In the general case, all μ_f may be different.

The solution of above equations of motion (6) with respect to the mean fields is

$$\zeta_f^2 = \eta^2 + \frac{N_g}{4N_c} \xi_f^2. \quad (12)$$

Here we heavily rely on the condition $N_c = N_f$. It is easy to verify [26] that with this solution the effective masses of gluons and quarks, cf. Eqs (3) and (4), reproduce the hard-thermal-loop results [27] in the high-temperature limit, provided the coupling constant $g^2(\chi)$ is appropriately defined. In fact, this property was the main requirement in construction of this DQ model [26]. The appropriate choice of the coupling constant [26] is the following

$$g^2(\chi) = \frac{16\pi^2}{\beta_0 \ln[(\chi^2 + \chi_0^2)/\chi_C^2]} f(\chi), \quad (13)$$

where $\beta_0 = \frac{1}{3}(11N_c - 2N_f^{\text{eff}})$. N_f^{eff} is the effective number of quark flavors at the energy scale χ , which may be $N_f^{\text{eff}} < N_f$ [49]. The parameter χ_C^2 is introduced in Eq. (5) and χ_0^2 is another phenomenological parameter of the model. An auxiliary function $f(\chi)$, satisfying the

condition $f(\chi \rightarrow \infty) \rightarrow 1$, helps us to choose between the 1-loop and 2-loop perturbative limits of the coupling constant [30, 31].

The “1-loop” version of the model

$$f_{1\text{-loop}} \equiv 1 \quad (14)$$

overestimates by approximately 10% the lattice data (see Ref. [26] and discussion in Sect. III). Therefore, the “2-loop” version was also considered. The latter was chosen in the form

$$f_{2\text{-loop}}(\chi) = 1 + \arctan \left[\frac{\beta_1}{8\pi^2 \beta_0} g^2(\chi) \ln \frac{g^2(\chi)}{\lambda} \right] \quad (15)$$

with

$$\beta_1 = \frac{1}{6}(34N_c^2 - 13N_c N_f^{\text{eff}} + 3N_f^{\text{eff}}/N_c), \quad \lambda = 0.001 \frac{16\pi^2}{\beta_0}.$$

With this $f_{2\text{-loop}}$, the coupling constant meets the 2-loop perturbative limit at $\chi \rightarrow \infty$. The additional $g^2 \ln(0.001)$ term is sub-leading as compared to $g^2(\chi) \ln g^2(\chi)$ and thus does not prevent agreement with the 2-loop approximation for the coupling constant. In fact, the function $f_{2\text{-loop}}$ is an “exotic” representation of a constant, since in the range, covered by lattice simulations, $f_{2\text{-loop}}(\chi) \simeq 2.6$ with good accuracy. Precisely this enhancement of the coupling constant is required to fit the actual overall normalization of the lattice results.

As we have mentioned the present model simulates the confinement of quarks and gluons. At some value of χ the argument of $\ln[(\chi^2 + \chi_0^2)/\chi_C^2]$ in Eq. (13) becomes very close to 1, and hence $g^2 \rightarrow \infty$. Due to that there are no solutions to the above equations below certain values of temperature and chemical potentials. This can be interpreted as a kind of confinement.

To summarize, the procedure of solving the model equations is as follows. First, we define all the free parameters of the model (χ_C, χ_0, B_C) , including the auxiliary function $f(\chi)$. Given the temperature T and the set of chemical potentials μ_f , the set of equations (2)–(4) and (7)–(13) should be solved. As a result of this solution, we obtain effective quark and gluon masses and the value of χ variable, which is required for calculation of $B(\chi)$, cf. Eq. (5). When all the quantities are defined, we can calculate the energy density $\varepsilon(T, \{\mu_f\})$, pressure $P(T, \{\mu_f\})$, and baryon density $n(T, \{\mu_f\})$ as follows

$$\begin{aligned}\varepsilon(T, \{\mu_f\}) &= \left(1 - \frac{4}{5}c\right) \frac{N_g}{2\pi^2} \int_0^\infty k^2 dk (k^2 + m_g^2)^{1/2} f_g(k) \\ &+ (1 - c) \sum_{f=1}^{N_f} \frac{N_c}{\pi^2} \int_0^\infty k^2 dk (k^2 + m_f^2)^{1/2} [f_f(k) + f_{\bar{q},f}(k)] + B(\chi) + \delta B_\Delta, \\ P(T, \{\mu_f\}) &= \left(1 - \frac{4}{5}c\right) \frac{N_g}{6\pi^2} \int_0^\infty \frac{k^4 dk}{(k^2 + m_g^2)^{1/2}} f_g(k)\end{aligned}\quad (16)$$

Version	T_C^a , MeV	m_u , MeV	m_d , MeV	m_s , MeV	m_g , MeV	$B^{1/4}$, MeV	c
light-bag-155	167	5	7	150	0	155	$0 \div 0.3$
light-bag-200	167	5	7	150	0	200	0
heavy-bag	167	330	330	450	600	183	$0 \div 0.3$

^aThe critical temperature T_C is chosen on the condition of the best reproduction of lattice predictions [12] by the “heavy-bag” model. For the “light-bag” models it was simply kept the same.

TABLE I: Parameters of bag models

$$+ (1-c) \sum_{f=1}^{N_f} \frac{N_c}{3\pi^2} \int_0^\infty \frac{k^4 dk}{(k^2 + m_f^2)^{1/2}} [f_f(k) + f_{\bar{q},f}(k)] - B(\chi) - \delta B_\Delta, \quad (17)$$

$$n(T, \{\mu_f\}) = \frac{1}{3} (1-c) \sum_{f=1}^{N_f} \frac{N_c}{\pi^2} \int_0^\infty k^2 dk [f_f(k) - f_{\bar{q},f}(k)]. \quad (18)$$

The gluon and antiquark terms vanish at zero temperature. Here we have introduced factors $(1 - \frac{4}{5}c)$ and $(1 - c)$ to make provision for the bag model (see the next Subsect.). For the DQ model, c is identically zero, $c_{\text{DQ-model}} \equiv 0$.

In Eqs (16) and (17) we have also made provision for a pairing contribution δB_Δ , which may be important at low temperatures. The respective term can be directly added to the Lagrangian. It preserves the above mean-field solution, provided it is independent of these mean fields. For temperature higher than a certain temperature T_c^{CSC} , this contribution vanishes, $\delta B_\Delta = 0$. For $T < T_c^{\text{CSC}}$ the quarks can be paired, forming a color superconductor. This gives rise to δB_Δ that depends on the color superconducting gap. The form of this term, δB_Δ , depends on the pairing channel. There exists a variety of possible phases. We will present the results for two phases usually discussed. One expects that the phase that can be realized at moderate densities is the two-color-superconducting (2SC) phase. At larger densities the most symmetric color-flavor-locked (CFL) phase may be formed (for $\Delta > 3m_s^2/(2\mu)$). In these cases we have [32]

$$\delta B_\Delta \simeq -\frac{\nu \Delta^2 \mu^2}{\pi^2} \quad \text{at} \quad T < T_c^{\text{CSC}}, \quad (19)$$

where $\Delta(T)$ is the gap, $\nu = 1/9$ for 2SC phase and $\nu = 1/3$ for CFL phase, and μ is the baryon chemical potential.

Note that thermodynamic consistency is automatically fulfilled in our scheme, since we proceed from a proper Lagrangian formulation. The presented model is of pure mean-field nature. In particular, it disregards fluctuations that may be important in the vicinity of both the deconfinement and the superconducting phase transitions [33]. However, these fluctuations are usually disregarded in other models applied to both high and low temperatures as well. These effects require further study.

B. Bag models

The last formulas of the previous subsection, i.e. Eqs (16)–(18), are directly applicable to the bag model with the only simplification that all masses m_u, m_d, m_s, m_g and the bag constant B are really constants, i.e. are independent of any mean fields, temperature and chemical potentials. Often perturbative corrections $\propto g^2$ to the kinetic terms of both quarks [34] and gluons [35] given by the factor c (which is $2\alpha_s^2/\pi$ in case of massless quarks and gluons) are also taken into account, see Eqs (16)–(18). Since perturbation theory is not applicable to the whole region of temperatures and chemical potentials of our interest, we will not use an explicit expression for this correction but rather vary it within a reasonable range, $c = 0 \div 0.3$, following Ref. [28].

Below we consider three versions of the bag model, the parameters are listed in Table I. The two first versions, labeled “light-bag-155” (similar to the model used in Ref. [28]) and “light-bag-200” (similar to the model used in Ref. [29]), represent a range of “conventional” bag models used in astrophysical applications. As we will show below these models cannot reproduce lattice results. The “heavy-bag”, as well as DQ based models, are fitted to reasonably reproduce lattice data of Ref. [12], see next section. This fit required heavy quarks and gluons to be introduced.

III. COMPARISON WITH LATTICE RESULTS

In this section we demonstrate the quality of the fit of the above described models to the recent (2+1)-flavor lattice predictions at various chemical potentials [12].

We again start with a brief recapitulation of Ref. [26], where this comparison was done for the DQ model. To be consistent with the lattice data, current quark masses

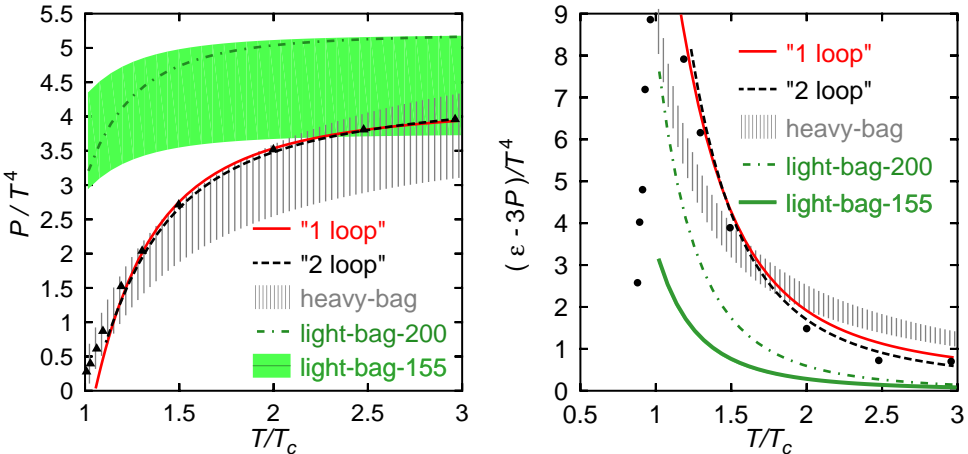


FIG. 1: Pressure (left panel) and the interaction measure, $\varepsilon - 3P$, (right panel) scaled by T^4 as functions of T/T_c at zero baryon chemical potential $\mu = 0$. The solid line corresponds to “1-loop” version, whereas the dashed line, to the “2-loop” one of the DQ model. The vertically hatched band is the “heavy-bag” fit with $c = 0$ and $c = 0.3$ for the top and bottom boundary lines, respectively. The grey band (for P) and the grey line (for $\varepsilon - 3P$) represent prediction of the “light-bag-155” model. The dash-dotted line corresponds to the “light-bag-200” model. Lattice data, triangles and dots, are from Ref. [12].

$m_{u0} = m_{d0} = 65$ MeV and $m_{s0} = 135$ MeV were adopted, as in these lattice calculations. It was found that the actual results of our quasiparticle model are quite insensitive to variation of m_{f0} from above lattice values to the “physical” ones $m_{u0} = m_{d0} = 7$ MeV and $m_{s0} = 150$ MeV. The model involves several phenomenological parameters: the parameter B_C , cf. (5), the “QCD scale” χ_C , and an auxiliary function $f(\chi)$, cf. (13). Another parameter χ_0^2 should be taken small $\chi_0^2 \ll \chi_C^2$. It shifts the lower limit of integration in the expression for $B(\chi)$, cf. Eq. (5), from the singular point of the coupling constant, cf. Eq. (13), and hence regularizes the calculation of $B(\chi)$. Therefore, it is closely related to the parameter B_C , which is an integration constant in the same expression. A change of χ_0^2 implies the corresponding change of B_C . In all further calculations we take $\chi_0^2 = 0.01\chi_C^2$, and the values of B_C stated below correspond only to this choice.

An implicit parameter of the model is the critical temperature T_C , i.e. the temperature at which the deconfinement phase transition occurs at $\mu = 0$. It would not be reasonable to identify this temperature with that of the end point of the solution discussed above. The reason is that the phase transition at $\mu = 0$ in the case of (2+1) flavors is of the cross-over type, as found in lattice calculations. This implies that a strong interplay between quark-gluon and hadronic degrees of freedom occurs near T_C , which actually determines the T_C value itself. Since hadronic degrees of freedom are completely disregarded in the model, it cannot properly determine the T_C value. Therefore, the value of T_C was varied from the determined end-point temperature to slightly below in order to achieve the best fit of the lattice results. The fitted value $T_C = 195$ MeV is slightly above its lattice counterpart 175 MeV.

As demonstrated in Ref. [26], the “1-loop” version of

Version	N_f^{eff}	T_C , MeV	χ_C , MeV	B_C/χ_C^4 ^a	f-factor ^b	N_{norm}
“1-loop”	3	195	141.3	-97.5	1	0.9
“2-loop”	3	195	119.6	-267.5	2.6	1

^aThese B_C values correspond to the choice $\chi_0^2 = 0.01\chi_C^2$.

^bThis is the effective value of the auxiliary function $f(\chi)$ in the temperature range under investigation, i.e. from T_C to $3T_C$.

TABLE II: Best fits of DQ-model parameters to lattice data [12]

the DQ model, cf. Eq. (14), does not reproduce the overall normalization of the lattice pressure. For the best fit of the lattice data the overall normalization factor (N_{norm}) was chosen equal 0.9 for the “1-loop” calculations. The value N_{norm} is indeed somewhat uncertain. Lattice calculations were done on lattices with $N_t = 4$ temporal extension [12]. To transform the “raw” lattice data into physical values, i.e. to extrapolate to the continuum case of $N_t \rightarrow \infty$, the raw data are multiplied by “*the dominant $T \rightarrow \infty$ correction factors between the $N_t = 4$ and continuum case*”, $c_p = 0.518$ and $c_\mu = 0.446$, [12]. These factors are determined as ratios of the Stefan-Boltzmann pressure at $\mu = 0$ (c_p) and the μ -dependent part of the Stefan-Boltzmann pressure (c_μ) to the corresponding values on the $N_t = 4$ lattice [12]. In view of this uncertainty, it is reasonable to apply an additional overall normalization factor N_{norm} to the same quantities calculated within DQ model [50]. In order to keep the number of fitting parameters as small as possible, a single normalization factor N_{norm} was applied instead of two different ones, c_p and c_μ , as in the lattice calculations.

As for the “2-loop” version, the auxiliary function (15) was chosen to reproduce the lattice data normalization. In fact, the function $f_{2\text{-loop}}$ is an “exotic” representation

of a constant, since in the temperature range under consideration, from T_C to $3T_C$, $f_{2\text{-loop}}(\chi) \simeq 2.6$ with good accuracy. In this respect, any function f , providing us with the additional factor 2.6 in the temperature range from T_C to $3T_C$ and respecting the proper perturbative limit of the coupling constant at very high temperatures, is just as suitable for this fit. The two sets of parameters of the DQ model are summarized in Table II.

The comparison with (2+1)-flavor lattice results [12] of the above two versions of the DQ model, as well as the various bag models of Table I, is presented in Figs. 1 and 2. The baryon chemical potential μ is defined as follows: $\mu_u = \mu_d = \mu/3$ and $\mu_s = 0$. *Both versions of the DQ model perfectly fit the lattice data above T_C .* This fact demonstrates that the way to fit these data even within the DQ model is not unique.

For two of the bag models we have taken into account the uncertainty associated with the perturbative correction c . Following Ref. [28] we varied c from 0 to 0.3, see Table I. Therefore, the results for bag models (“light-bag-155” and “heavy-bag”) are displayed, as a rule, by bands with $c = 0$ and $c = 0.3$ for the top and bottom boundary lines, respectively. In the case of the “interaction measure” $\epsilon - 3P$ and light quarks, the kinetic terms cancel with good accuracy and the band shrinks to a line. For the “light-bag-200” model, we do not display uncertainties associated with c in order not to overload the figure and since the general picture seems clear without this additional variation: *the “light-bag” models do not follow lattice predictions.* We checked that these fits to the pressure and “interaction measure” $\epsilon - 3P$ could be improved at the price of a significant increase of the bag constant B . However, reproduction of these lattice quantities still remains rather poor even with this improvement. Moreover, the remaining quantities, ΔP and n_B , prove to be unchanged, since they are independent of B . Within the above mentioned c -uncertainty, *the “heavy-bag” model reasonably well covers the lattice data, however, at expense of introducing large quark and gluon constituent masses.*

To reveal similarities between the DQ and bag models, in Fig. 3 we compare quark/gluon masses and bag parameters from these two kinds of models. Note that these are the only quantities that matter in the calculations of thermodynamic functions such as those of Eqs (16)–(18). The u and d quark masses of the DQ model are indistinguishable within the scale of this figure. Quark and gluon masses, required for the reproduction of the lattice results, are high ($\gtrsim 300$ MeV) in both the DQ model and the “heavy-bag” model. Thus, *the failure of the “light-bag” models to reproduce lattice data can be associated with the light quark and gluon masses used in the calculation.* Note that in the DQ model, B becomes negative at high temperatures. This means that the interaction changes from repulsion to attraction. This behavior of the bag parameter is common for models reproducing lattice data, cf. Refs [18, 21].

As argued in Ref. [36], the lattice data below T_C are

well reproduced by the resonance hadronic gas model. However to comply with the lattice results, hadron masses in this resonance hadronic gas should be enhanced. In particular, the pion mass was taken $m_\pi \simeq 770$ MeV, as resulted from lattice calculations. This fact indicates that the EoS in the hadronic sector is not reliably predicted by the lattice calculations. The analysis of Ref. [37] shows that strong interaction effects might be crucially important in the description of the hadron system at high temperatures and small baryon chemical potentials. Also we cannot use the resonance hadronic gas model at the low temperatures of present interest due to the lack of interactions incorporated in this model. This is why we avoid fitting our realistic hadronic EoS’s, discussed in the next section, to the lattice data.

IV. EOS AT $T = 0$: HYBRID AND QUARK STARS

A. Cold matter in β equilibrium

For matter in β -equilibrium at zero temperature several conditions should be met. Chemical potentials of quarks and leptons satisfy equilibrium conditions with respect to reactions $u + e \leftrightarrow s$, $d \leftrightarrow s$, $\mu \leftrightarrow e$:

$$\mu_u + \mu_e = \mu_s, \quad \mu_d = \mu_s, \quad \mu_\mu = \mu_e. \quad (20)$$

The baryon (neutron) chemical potential is related to the quark chemical potentials as

$$\mu \equiv \mu_n = 2\mu_d + \mu_u. \quad (21)$$

As argued in Ref. [38], the region of the hadron-quark mixed phase is very narrow, if not absent, due to rather high surface tension and charge screening effects on the quark-hadron boundary. Therefore, we can use a Maxwell construction in order to describe the quark-hadron phase transition. This implies the local electro-neutrality

$$\frac{2}{3}n_u - \frac{1}{3}n_d - \frac{1}{3}n_s - n_e - n_\mu = 0, \quad (22)$$

where n_u , n_d , n_s are quark densities, n_e is the electron density and n_μ is the muon density. The lepton contribution to the pressure is given by

$$P_l = \sum_{i=e,\mu} \left[n_i \mu_i - \int_0^{p_{Fi}} \frac{p^2 dp \sqrt{p^2 + m_i^2}}{\pi^2} \right], \quad (23)$$

where m_e and m_μ are lepton masses, $\mu_i = \sqrt{p_{Fi}^2 + m_i^2}$, e and μ densities are

$$n_i = \frac{(\mu_i^2 - m_i^2)^{3/2}}{3\pi^2} \theta(\mu_i - m_i), \quad (24)$$

and $\theta(x)$ is the ordinary step function.

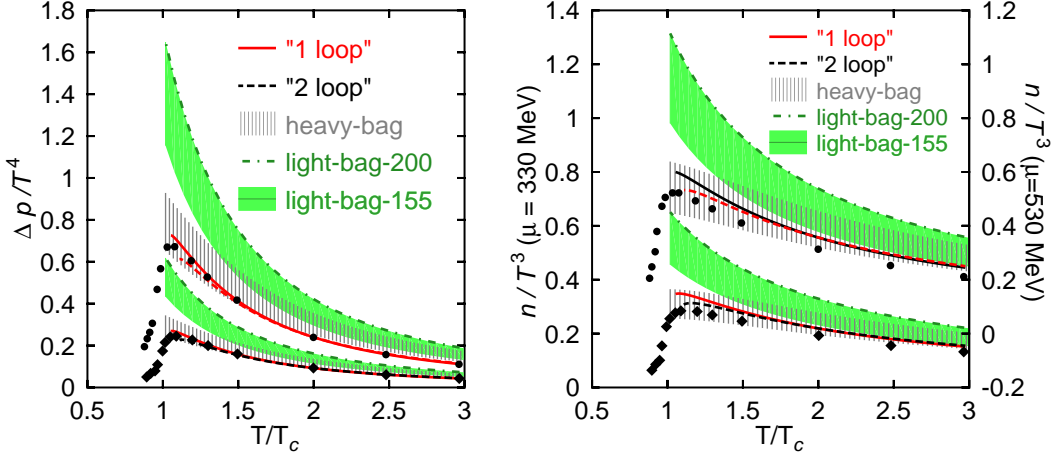


FIG. 2: $\Delta P = P(T, \mu) - P(T, \mu = 0)$ (left panel) and the baryon density n (right panel) scaled by T^4 and T^3 as functions of T/T_c at nonzero baryon chemical potentials $\mu = 330$ and 530 MeV (from bottom to top). Note different scales (left and right, respectively) for $\mu = 330$ and 530 MeV in the right panel. Notation is the same as in Fig. 1.

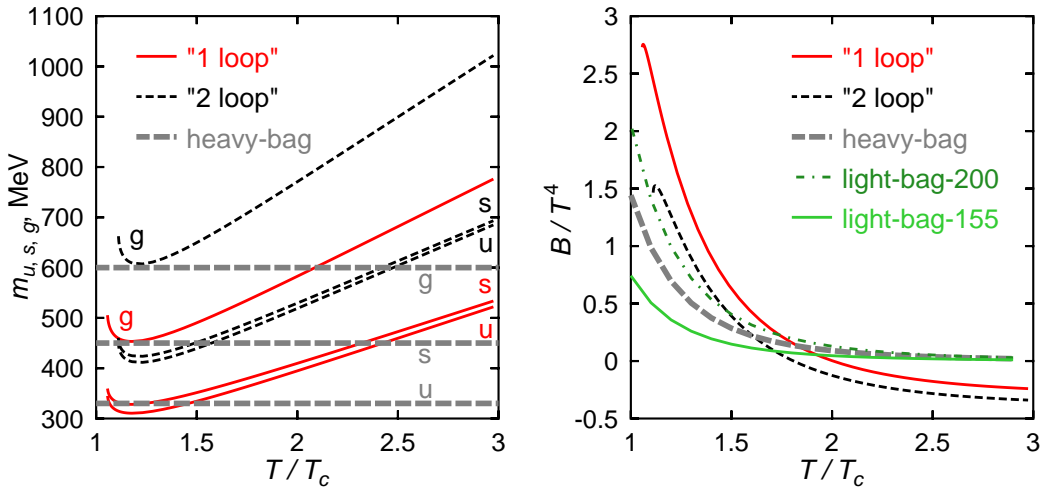


FIG. 3: Quark and gluon effective masses (left panel) and bag parameters scaled by T^4 (right panel) for the DQ model, cf. Eq. (5), and bag models as functions of T/T_c at zero baryon chemical potential $\mu = 0$. Notation is the same as in Fig. 1.

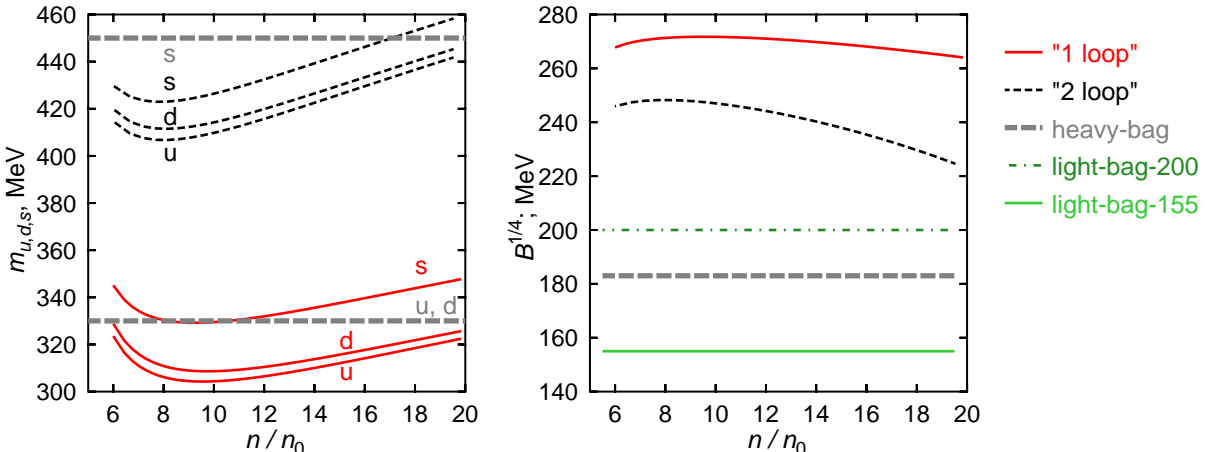


FIG. 4: Effective quark masses (left panel) and bag parameters (right panel) for the DQ models (curves), cf. Eq. (5), and bag models (horizontal lines) as functions of n/n_0 for $T = 0$ at β equilibrium. Notation is the same as in Fig. 1.

Now let us specify the hadronic EoS. The Urbana–Argonne EoS [39] $A18 + \delta v + UIX^*$ complies with the rich experimental information available for $n \lesssim n_0$ (n_0 is the nuclear saturation density). For that reason this EoS is considered to be the most realistic EoS at present. However, it uses a non-relativistic potential and hence violates causality at $n \gtrsim 4n_0$. Ref. [29] suggested a simple analytical parameterization (below referred as the HHJ EoS) of $A18 + \delta v + UIX^*$ EoS valid for $n \lesssim 4n_0$, which respects causality at higher densities. On the other hand, as an extrapolation to higher densities, relativistic mean field (RMF) models are practical. However all RMF models have an unpleasant feature. They produce a large fraction of protons in neutron star matter that permits a very efficient cooling process, i.e. the direct Urca (DU) process $n \rightarrow pe\bar{\nu}$, for rather low densities $< 3n_0$. First, this disagrees with predictions of the mentioned $A18 + \delta v + UIX^*$ EoS, where the DU process is allowed only for $n > 5n_0$. Second, a low threshold density $n_{\text{crit}}^{\text{DU}} \lesssim 3n_0$ seems to be at odds with a neutron star cooling scenario [40] predicted by the Urbana–Argonne EoS.

Another problem is that rather massive neutron stars may exist. Recent measurements of neutron star masses in binary compact systems yielded $M_{\text{J0751+1807}} = 2.2 \pm 0.2M_{\odot}$ [41] at the 95% confidence level. Even assuming the highest value of the uncertainty of this measurement one can conclude that $M_{\text{J0751+1807}} > 1.6M_{\odot}$ (within 2σ). Some models with a so-called soft hadron EoS do not satisfy this requirement. Note that the Urbana–Argonne EoS yields the limiting mass of a neutron star $\simeq 2.2M_{\odot}$. With the relativistic HHJ EoS the limiting neutron star mass decreases slightly below $\simeq 2M_{\odot}$. Possible phase transitions to the either pion or kaon condensation, hyperonization, quark matter, etc. soften the EoS, that may significantly decrease the limiting mass of the star, cf. Ref. [42].

Ref. [43] suggested a solution of both problems within an effective RMF model with field dependent effective hadron masses and coupling constants. We will use two models from this work. One model, “hadron-MW2” (MW(nu)(z = 2.6) in the notation of Ref. [43]), fits the HHJ EoS for all densities yielding the threshold density for the DU process $\simeq 5.2n_0$. Another model, “hadron-MW1” (MW(nu)(z = 0.65) in the notation of Ref. [43]) fits the HHJ EoS for $n \lesssim 2n_0$ but allows an increase the limiting mass of a neutron star due to a stiffening of the EoS at a higher density. The threshold of the DU process is $\simeq 4n_0$ which does not contradict to the above mentioned description of the star cooling. Thus, the “hadron-MW1” model possesses the same advantages, as the Urbana–Argonne EoS and the “hadron-MW2” one, but in addition allows an increase the limiting mass of the star. The pressure of the “hadron-MW1” model as a function of the baryon chemical potential is lower as compared to that of the “hadron-MW2” model, which is in favor of the phase transition to the quark state at a smaller density. In order to keep the considerations sim-

ple, we use models that disregard the possibility of ρ^- condensation discussed in Ref. [43].

In Fig. 4 (left panel) we show effective masses of quarks at $T = 0$ as a function of the baryon density in units of the normal nuclear matter density $n_0 \simeq 0.16 \text{ fm}^{-3}$. Horizontal lines represent quark masses of the “heavy-bag” model, see Table I. Self-consistent calculations of the DQ model produce a much smaller difference between strange and non-strange quark masses compared to 120–150 MeV, which is usually accepted by bag models. In the DQ model, quark masses slightly decrease with increasing density up to $(8 \div 9)n_0$. For higher densities the behavior reverses and the masses undergo a slight increase. Note that such a density behavior of the quark masses is quite different from that obtained in the NJL model [44]. In the latter case for zero temperature the quark masses drop with increasing density, reaching zero at a moderate value of the baryon density n_c , they also drop to zero at $T = T_C$. Therefore it seems doubtful that the NJL model could reproduce the lattice data at least near and above T_C ; similarly we have shown that the “light-bag” models fail.

Fig. 4 (right panel) demonstrates the behavior of the effective bag parameter $B^{1/4}$ as a function of density at zero temperature. The B values prove to be very high in the DQ model, whereas the bag parameter of the “heavy-bag” model is in the range of ordinarily used values.

B. Do hybrid stars exist?

In Fig. 5 we present the pressure as a function of the baryon chemical potential (left panel) and as a function of the baryon density (right panel) for the models considered above. Realistic hadronic RMF EoS’s are represented by the “hadron-MW2” and “hadron-MW1” models discussed above. The latter EoS is stiffer, as is seen from the right panel. As a reference model, the stiffest RMF EoS of the original Walecka model (“hadron-W”) is also demonstrated. The crossing points of the hadronic and quark curves on the (P, μ) plane (left panel) show critical values (μ_c, P_c) for occurrence of the first-order phase transition from the hadronic to the quark phase. The latter transition arises, if for $\mu > \mu_c$ the pressure of the quark phase is higher than that for the hadron phase. The corresponding critical densities n_c^h and n_c^q at the Maxwell construction, $n_c^h < n_c^q$, are listed in Table III.

As seen, all lattice-QCD-motivated models (DQ and “heavy-bag”) of the quark phase matched with realistic RMF models (either “hadron-MW1” or “hadron-MW2”) of the hadronic phase predict the onset of the phase transition at very high critical densities (typically $n_c^h \sim 10n_0$). Note that both “hadron-MW1” and “hadron-MW2” models do not permit neutron stars with central baryon densities $\geq 8n_0$, see Ref. [43]. *Thus, our lattice-QCD-motivated models (DQ and “heavy-bag”) matched with realistic RMF models (either “hadron-*

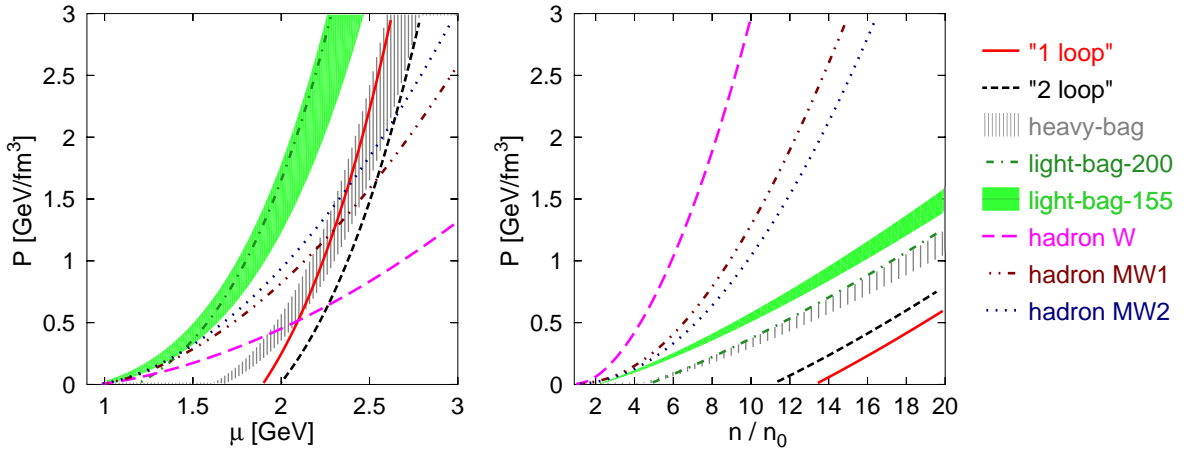


FIG. 5: Pressure as a function of the chemical potential (left panel) and n/n_0 (right panel) for $T = 0$ at β equilibrium. Notation for the quark models is the same as in Fig. 1. Band boundaries for the “heavy-bag” and “light-bag-155” model correspond to $c = 0$ and $c = 0.3$: from top to bottom in left panel and from bottom to top in right panel. Hadronic EoS of the conventional Walecka model (“hadron W”) is displayed by long-dashed line. Two versions of the hadronic model of Ref. [43], i.e. “hadron-MW1” and “hadron-MW2”, are presented by dashed-dotted-dotted and dotted lines, respectively.

“MW1” or “hadron-MW2”) do not allow the existence of hybrid stars. The stiffer the hadron EoS, the lower the critical density n_c^h is. However, the central density of the limiting mass star also decreases. In the case of the DQ and “heavy-bag” models matched with the “hadron-W” model representing unrealistically stiff EoS (i.e. the stiffest EoS among those still used in calculations), the typical critical density $n_c^h \approx 4n_0$. The critical masses $M(n_{cent} = n_c^h)$ for the occurrence of the hybrid stars are listed in Table IV. Three hadron-quark model combinations, i.e. “hadron-W”+“1-loop” and “hadron-W”+“heavy-bag” with $c = 0$ and $c = 0.3$, predict the existence of hybrid stars with $M > 2.7 M_\odot$. These mass values are only slightly below the limiting mass. The hadron-quark combination “hadron-W”+“2-loop” predicts no hybrid stars.

The “light-bag-155($c = 0.3$)” and “light-bag-200($c = 0$)” models result in critical densities in a range which is usually considered in papers devoted to hybrid stars. For the “light-bag-155($c = 0$)” model matched with any of the considered hadron models, quark matter is always more stable than hadronic matter (the quark pressure is higher), and hence quark stars of an arbitrary size are possible. In this case only a softer (compared to those we have used) hadronic EoS could allow the possibility of hybrid star existence.

C. Quark stars

Now we turn to the question of the possible existence of pure quark stars. We assume the absence of a hadronic shell and for simplicity disregard presence of a crust. The latter is indeed tiny, if any, in the case of quark stars, see Ref. [10]. To solve the Oppenheimer-Volkoff equation we need the $\varepsilon(P)$ dependence. The pressure as a function

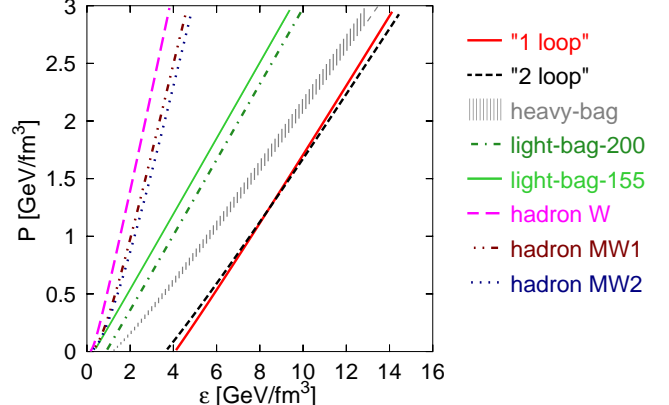


FIG. 6: Pressure versus energy density at $T = 0$ in β -equilibrium for various EoS’s. Band boundaries for the “heavy-bag” model correspond $c = 0$ and $c = 0.3$ (from bottom to top). Notation is the same as in Figs 1 and 5.

of the energy density is shown in Fig. 6 for the models under consideration. We see that for all the quark models these dependencies can be well parameterized with appropriate accuracy by straight lines $\varepsilon = aP + b$, with $b = 4\tilde{B}$, where \tilde{B} has the meaning of an effective bag parameter, cf. Ref. [19, 20]. For the “massless-bag” model, i.e. with all quarks being massless, we would obtain $a = 3(1 - c)$, $b = 4B$. Values of the effective bag parameter \tilde{B} and slop-coefficients “ a ” are listed in Table V. Note that the quasiparticle model of Refs [19, 20] resulted in $3.1 \leq a \leq 4.5$ and $\tilde{B}^{1/4} > 200$ MeV (typically $\tilde{B}^{1/4} \simeq (230 \div 240)$ MeV). Within our lattice-QCD-motivated models (DQ and “heavy-bag”) we obtained essentially higher values: $a = 5 \div 6$ for and $\tilde{B}^{1/4} = 212 \div 304$ MeV. As seen, the $\varepsilon(P)$ lines are quite different for the

hadr.\ quark	“1-loop”	“2-loop”	heavy-bag($c = 0$)	heavy-bag(0.3)	light-bag-155(0.3)	light-bag-200(0)
W	4.4/20.3	4.8/19.3	3.9/12.1	4.4/12.6	1.3/2.6	2.2/6.4
MW1	9.8/27.7	11.2/29.7	9.3/22.0	10.8/24.1	3.7/4.3	4.4/7.1
MW2	12.2/31.3	14.1/34.5	11.5/25.1	13.7/29.1	5.8/7.1	5.4/9.1

TABLE III: The hadronic n_c^h and quark n_c^q critical densities (in units n_0) according to the Maxwell construction.

hadr.\ quark	“1-loop”	“2-loop”	heavy-bag($c = 0$)	heavy-bag(0.3)	light-bag-155(0.3)	light-bag-200(0)
W	2.7	—	2.8	2.7	0.6	2.1
MW1	—	—	—	—	1.6	1.8
MW2	—	—	—	—	1.8	1.7

TABLE IV: Masses of neutron stars M (in units M_\odot) corresponding to the critical densities in the hadron phase, n_c^h , listed in Table III.

“light-bag”, “heavy-bag” and DQ models. Due to that one may expect quite different gravitational properties of objects described by these models.

In Fig. 7 we show mass-radius (M – R) relation for our models of quark stars. Two extreme cases are demonstrated: quark matter in the normal phase (left panel) and the CFL phase of quark matter with a high pairing gap $\Delta = 100$ MeV (right panel). In the latter case the contribution of pairing to the energy density is the largest. For other superconducting phases, the results will range in between these two extremes presented here. Note that occurrence of high n_c^q values in our DQ and “heavy-bag” models, see Table III, implies that the CFL phase takes place in these cases. Fig. 8 demonstrates the quark star mass as a function of the central baryon density, again for the normal phase with $\Delta = 0$ (left panel) and the CFL phase with $\Delta = 100$ MeV (right panel). The limiting masses and central densities are listed in Table VI for normal quark matter and in Table VII for the CFL quark matter. Note that CFL strangelets were discussed in Ref. [45].

In the case of “light-bag-155” model the pairing may substantially affect the EoS and hence quark star masses. The difference between normal and CFL quark star masses increases up to $0.6 M_\odot$ in the region $M \sim M_{lim}$. The limiting mass is $M_{lim} \sim (1.6 \div 2.3) M_\odot$ and the radius is $\sim 9 \div 12$ km. Thus, for these models the M – R and M – n_{cent} relations are similar to those one usually uses for pure hadronic EoS’s, in agreement with the statement of Ref. [28]. For the “light-bag-200($c = 0$)” model the limiting mass is $M_{lim} \sim (0.9 \div 1.2) M_\odot$ and the radius is ~ 6 km. This limiting mass is smaller than several well measured masses of pulsars. Thus we may conclude that the “light-bag-200” model does not describe ordinary pulsars but rather another family of compact objects. The effect of the pairing is less pronounced here than for the “light-bag-155” model. Let us remind that the “light-bag-155($c = 0.3$)” and “light-bag-200($c = 0$)” models matched with either “hadron MW1” or “hadron MW2” hadronic models also predict existence of hybrid

stars. Had we assumed a softer hadron EoS, the corresponding hybrid stars would become impossible and we would only have pure quark stars.

For the “heavy-bag” model and especially for the DQ model, the masses and radii are still smaller and the interior region, denser. For the “heavy-bag” model the limiting mass is $M \sim (0.6 \div 1) M_\odot$ and the radius is $(\sim 4 \div 6)$ km. These configurations are similar to those previously studied in the model of Ref. [20]. For the DQ model the limiting mass is $M \sim (0.4 \div 0.5) M_\odot$ and the radius is $(\sim 2.5 \div 3)$ km. The central density is $\sim (50 \div 60) n_0$. Such dense quark matter is probably realized in the CFL phase that has peculiar cooling properties. Small and dense objects might be of interest with respect to MACHO events [46].

V. CONCLUSIONS

Models for deconfined quark matter are extensively used in astrophysical applications. The discussion of hypothetical hybrid and quark stars is a rather hot topic. In this paper we emphasize that it is essential for a deconfined quark model to be constrained by the lattice QCD results, which became recently available at finite baryon chemical potential. Rapidly progressing lattice calculations may essentially restrict models used for the description of cold and dense quark matter. In this paper we are trying to make a step in this direction. At this time, we would like to draw attention to problems with traditionally used simple standard bag and, probably, NJL models. They are not able to reproduce the lattice data without significant modifications.

We have considered the dynamical quasiparticle model [26] and the heavy-bag model, which fit the lattice results. The heavy-bag model uses heavy masses of quarks and gluons to reproduce the lattice results well. We have demonstrated, that these models, being matched with realistic hadron models of EoS, rule out the existence of hybrid stars. This implies that families

Model	“1-loop”	“2-loop”	heavy-bag($c = 0$)	heavy-bag(0.3)	light-bag-155(0)	light-bag-155(0.3)	light-bag-200(0)
a	5.01	5.97	5.89	5.41	3.11	3.09	3.15
$\tilde{B}^{1/4}$, MeV	304	293	216	212	159	159	202

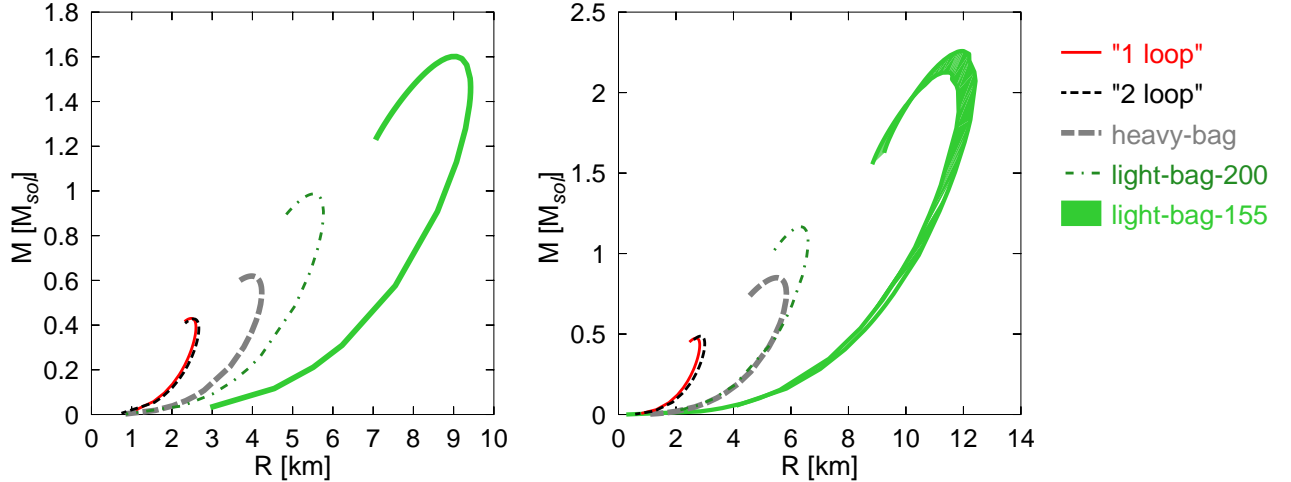
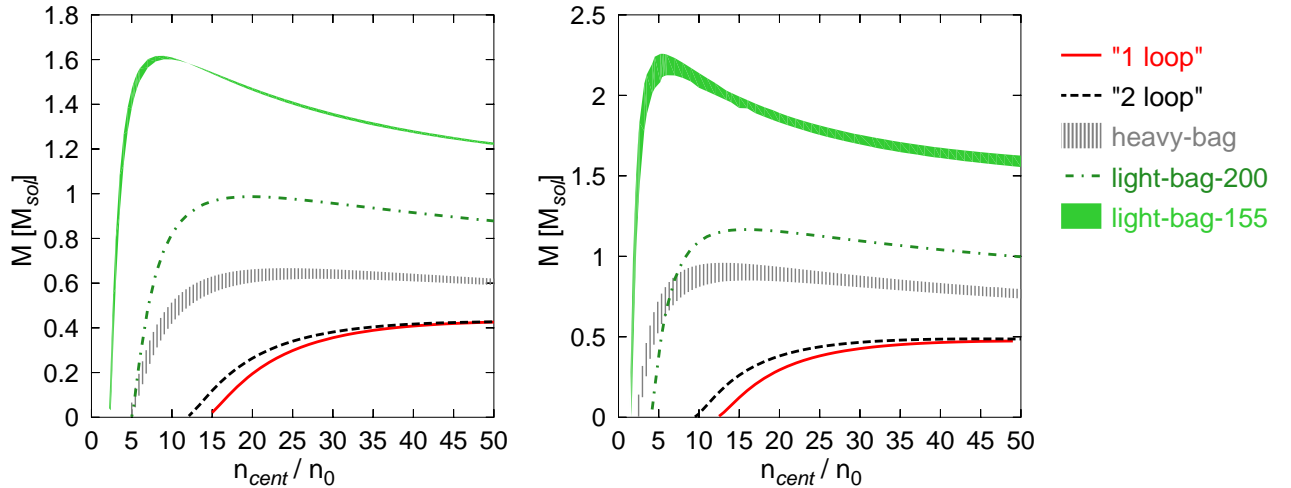
TABLE V: Coefficients of the linear interpolation of the $\varepsilon(P)$ dependence.FIG. 7: Quark star mass – radius relation of pure quark stars for the normal quark phase with $\Delta = 0$ (left panel) and the CFL quark phase with $\Delta = 100$ MeV (right panel). Notation is the same as in previous figures. Band boundaries $c = 0$ and $c = 0.3$, from bottom to top.

FIG. 8: Quark star mass – central density relation. Notation is the same as in Fig. 7.

Model	“1-loop”	“2-loop”	heavy-bag($c = 0$)	heavy-bag(0.3)	light-bag-155(0)	light-bag-155(0.3)	light-bag-200(0)
M_{lim}	0.43	0.43	0.62	0.67	1.60	1.62	0.99
n_{centr}	61.0	55.6	28.3	24.3	9.42	8.54	19.8

TABLE VI: Limiting quark star masses (in units M_\odot) and corresponding central densities (in units n_0) for the normal phase ($\Delta = 0$) of quark matter.

Model	“1-loop”	“2-loop”	heavy-bag($c = 0$)	heavy-bag(0.3)	light-bag-155(0)	light-bag-155(0.3)	light-bag-200(0)
M_{lim}	0.47	0.49	0.85	0.96	2.13	2.26	1.17
n_{centr}	53.2	46.9	16.1	13.0	6.41	5.02	15.8

TABLE VII: The same as Table VI but for the CFL phase of quark matter with $\Delta = 100$ MeV.

of ordinary neutron stars and pure quark stars are well separated. Within these models the quark stars have low masses ($M \lesssim 1 M_{\odot}$), are dense ($n \gtrsim 10n_0$) and very compact ($R \lesssim 6$ km). This result complies with that obtained in Ref. [20] by means of a different extrapolation of lattice data to cold dense baryonic matter. If such a quark star existed in a binary system (together with a white dwarf, a neutron star, or together with another quark star), the orbiting would be different from that experimentally known for both white dwarf–neutron star and double neutron star systems. Moreover, such dense quark matter may be in the color-flavor-locked superconducting phase and hence possess peculiar cooling properties. Other properties of these pure quark stars also differ from those of neutron stars that may give a chance to distinguish them experimentally, e.g., see Ref. [45].

Another interesting question arises, what could be a possible formation mechanism of such compact and dense quark stars? Indeed, the models, which we fitted to lattice predictions, allow neither hybrid stars nor quark self-bound objects (strangelets). For the birth of a quark star, a hybrid star configuration is first required in order to produce a quark core either during supernova collapse or during the long-term accretion of the matter in a binary system, or in the course of the merging of two neutron stars. Then also a mechanism to blow off the hadron shell is need. We have demonstrated that only the unrealistically stiff original Walecka model (“hadron-W”) matched with either the DQ or “heavy-bag” models may allow for a small quark core. Thus, we actually see no appropriate mechanism to form quark stars that are described by our DQ and heavy-bag models. Temperature and neutrino trapping effects should be included. They may stiffen the hadron EoS and perhaps may help to resolve the problem. Some exotic ways to produce quark stars through either evolution of white dwarfs or inflation stage at the quark–hadron phase transition are discussed in Refs [46, 47]. Certainly, this problem still needs further consideration.

It is necessarily to mention uncertainties in the present considerations and the conclusions derived. First of all, they are connected with lattice data [12], which we extrapolate to the domain of cold and dense baryonic matter. These data obtained on a discrete lattice are only poorly extrapolated to the continuum limit. Another problem with the lattice data consists in the poor reproduction of the chiral limit. As we have mentioned already, the pion turns out to be very heavy in lattice calculations, e.g. $m_{\pi} \simeq 770$ MeV [36]. All this may result in certain errors in the parameters of our effective models, deduced

from these data. We have tried to estimate this kind of uncertainties by applying different extrapolations from the lattice data, i.e. the “1-loop” and “2-loop” versions of the DQ model and the “heavy-bag” model. Indeed, whereas the “2-loop” version closely reproduces the lattice data [12], the “1-loop” version slightly (by 10%) misfits its normalization, thus leaving room for uncertainty in the extrapolation to the continuum and chiral limits. As for the “heavy-bag” model, it covers the lattice data by a rather broad band (due to variation of c).

On the other hand, the grounds for the standard bag model, in our case represented by the “light-bag-155” and “light-bag-200” models, are not entirely reliable. Indeed, the bag parameters of standard bag models are fitted to reproduce the masses of hadrons, i.e. few-body systems, and then applied to describe matter. It could happen that the situation here is similar to that of Walecka model for nuclear matter. If we fit the Walecka model to reproduce the deuteron or helium and then apply it to ^{208}Pb , we surely get nonsense. Therefore, predictions of these models for the EoS should be treated with great care.

Theoretical uncertainties in our predictions should be mentioned as well. We cannot, of course, exclude that our models are oversimplified and some important physics is left aside, e.g., thermal fluctuations are not included, which may play an important role in the vicinity of the critical temperature but die out at smaller and higher temperatures. This may somehow modify the fitting parameters of models. Quantum fluctuations like instantons and gluon condensate may partially survive and additionally contribute in the low temperature region, cf. Ref. [48]. Thus, it might well be that the DQ model, as well as the heavy-bag model, should be replaced in the future by more sophisticated and realistic microscopically based models. Nevertheless, a certain confidence in our results is supported by the fact that another independent extrapolation of the lattice data to the cold dense baryonic matter [20] resulted in rather similar conclusions. However, it would be of interest to search for new theoretical approaches for extrapolating the EoS from $T > 190$ MeV to $T = 0$ and from $\mu = 530$ MeV upwards.

Acknowledgments

We are grateful to P.J. Ellis for fruitful discussions and careful reading the manuscript. This work was supported in part by the Deutsche Forschungsgemeinschaft (DFG project 436 RUS 113/558/0-2), the Russian Foundation for Basic Research (RFBR grant 03-02-04008) and Rus-

sian Minpromnauki (grant NS-1885.2003.2). The work of E.E.K. was supported in part by the US Department of

Energy under contract No. DE-FG02-87ER40328.

[1] E. Shuryak, J. Phys. G **30**, S1221 (2004); M. Gyulassy, and L. McLerran, e-Print Archive: nucl-th/0405013.

[2] D. Ivanenko and D.F. Kurdelaizde, Lett. Nuovo Cim. **2**, 13 (1969); N. Itoh, Prog. Theor. Phys. **44**, 291 (1970).

[3] F. Weber, astro-ph/0407155; H. Heiselberg and V.R. Pandharipande, Ann. Rev. Nucl. Part. Sci. **50**, 481 (2000).

[4] K. Rajagopal and F. Wilczek, hep-ph/0011333.

[5] I. Bombaci, Nucl. Phys. A **681**, 205 (2001).

[6] J. Madsen, Phys. Rev. Lett. **85**, 10 (2000); A. Drago, A. Lavagno, and G. Pagliara, astro-ph/0312009.

[7] D. Blaschke, T. Klähn, and D.N. Voskresensky, Ap. J. **533**, 406 (2000); D. Page, M. Prakash, J.M. Lattimer, and A. Steiner, Phys. Rev. Lett. **85**, 2048 (2000); D. Blaschke, H. Grigorian, and D.N. Voskresensky, Astron. & Astrophys. **368**, 561 (2001); astro-ph/0403171; astro-ph/0411619.

[8] M. Buballa, hep-ph/0402234.

[9] A.R. Bodmer, Phys. Rev. D **4**, 1601 (1971); E. Witten, Phys. Rev. D **30**, 272 (1984).

[10] C. Alcock, E. Farhi, and A. Olinto, Ap. J. **310**, 261 (1986).

[11] F. Karsch, Lect. Notes in Phys. **583**, 209 (2002).

[12] Z. Fodor, Nucl. Phys. A **715**, 319 (2003); F. Csikor, G.I. Egri, Z. Fodor, S.D. Katz, K.K. Szabo, and A.I. Toth, JHEP **405**, 46 (2004).

[13] C.R. Allton, S. Ejiri, S.J. Hands, O. Kaczmarek, F. Karsch, E. Laermann, and C. Schmidt, Phys. Rev. D **68**, 014507 (2003).

[14] R.V. Gavai and S. Gupta, Phys. Rev. D **68**, 034506 (2003).

[15] M.I. Gorenstein and S.N. Yang, Phys. Rev. D **52**, 5206 (1995).

[16] W. Greiner and D.H. Rischke, Phys. Rep. **264**, 183 (1996).

[17] P. Levai and U. Heinz, Phys. Rev. C **57**, 1879 (1998).

[18] A. Peshier, B. Kämpfer, O.P. Pavlenko, and G. Soff, Phys. Rev. D **54**, 2399 (1996); A. Peshier, B. Kämpfer, and G. Soff, Phys. Rev. D **66**, 094003 (2002).

[19] A. Peshier, B. Kämpfer, and G. Soff, Phys. Rev. C **61**, 045203 (2000).

[20] A. Peshier, B. Kämpfer, and G. Soff, hep-ph/0106090.

[21] R.A. Schneider and W. Weise, Phys. Rev. C **64**, 055201 (2001); T. Renk, R.A. Schneider, and W. Weise, Phys. Rev. C **66**, 014902 (2002).

[22] A. Rebhan and P. Romatschke, Phys. Rev. D **68**, 025022 (2003).

[23] K.K. Szabó and A.I. Tóth, JHEP **306**, 008 (2003).

[24] M.A. Thaler, R. Schneider, and W. Weise, Phys. Rev. C **69**, 035210 (2004).

[25] M. Bluhm, B. Kampfer, and G. Soff, hep-ph/041106.

[26] Yu.B. Ivanov, V.V. Skokov, and V.D. Toneev, accepted to Phys. Rev. D, hep-ph/0410127.

[27] E. Braaten and R.D. Pisarski, Phys. Rev. D **45**, R1827 (1992); J. Frenkel and J.C. Taylor, Nucl. Phys. B **374**, 156 (1992); J.P. Blaizot and E. Iancu, Nucl. Phys. B **417**, 608 (1994); J.O. Andersen, E. Braaten, and M. Strickland, Phys. Rev. Lett. **83**, 2139 (1999); Phys. Rev. D **62**, 045004 (2000); J.O. Andersen, E. Braaten, E. Petitgirard, and M. Strickland, Phys. Rev. D **66**, 085016 (2002); J.P. Blaizot, E. Iancu, and A. Rebhan, Phys. Rev. Lett. **83**, 2906 (1999); Phys. Lett. B **470**, 181 (1999); Phys. Rev. D **63**, 065003 (2001).

[28] M. Alford, M. Braby, M. Paris, and S. Reddy, nucl-th/0411016.

[29] H. Heiselberg, and M. Hjorth-Jensen, astro-ph/9904214; Phys. Rep. **328**, 237 (2000).

[30] J.I. Kapusta, *Finite-Temperature Field Theory*, Cambridge University Press, Cambridge, 1989.

[31] F.J. Yndurain, *The Theory of Quark and Gluon Interactions*, Berlin, Springer-Verlag, 1993.

[32] I.A. Shovkovy, nucl-th/0410091.

[33] D.N. Voskresensky, Phys. Rev. C **69**, 065209 (2004).

[34] T. DeGrand, R.L. Jaffe, K. Johnson, and J. Kiskis, Phys. Rev. D **12**, 2060 (1975).

[35] C.-X. Zhai and B.M. Kastening, Phys. Rev. D **52**, 7232 (1995).

[36] F. Karsch, K. Redlich, and A. Tawfik, Eur. Phys. J. **C29**, 549 (2003).

[37] D.N. Voskresensky, Nucl. Phys. A **744**, 378 (2004).

[38] D.N. Voskresensky, M. Yasuhira, and T. Tatsumi, Phys. Lett. B **541**, 93 (2002); Nucl. Phys. A **723**, 291 (2003); Toshiki Maruyama, T. Tatsumi, D.N. Voskresensky, T. Tanigawa, and S. Chiba, AIP Conf. Proc. **704**, 519 (2004); nucl-th/0311076.

[39] A. Akmal, V.R. Pandharipande, and D.G. Ravenhall, Phys. Rev. C **58** 1804 (1998).

[40] D. Blaschke, H. Grigorian, and D.N. Voskresensky, Astron. & Astrophys. **424**, 979 (2004).

[41] I.H. Stairs, Science, **304**, 547 (2004); D.J. Nice, E.M. Splaver, and I.H. Stairs, astro-ph/0411207.

[42] A. B. Migdal, E. E. Saperstein, M. A. Troitsky, and D.N. Voskresensky, Phys. Rep. **192**, 179 (1990); N. K. Glendenning, Phys. Rep. **342**, 393 (2001).

[43] E.E. Kolomeitsev and D.N. Voskresensky, nucl-th/0410063.

[44] S.P. Klevansky, Rev. Mod. Phys. **64**, 649 (1992).

[45] J. Madsen, Phys. Rev. Lett. **87**, 172003 (2001).

[46] E. Fraga, R.D. Pisarski, J. Schaffner-Bielich, Phys. Rev. D **63**, 121702 (2001).

[47] N. Borghini, W.N. Cottingham, and R. Vinh Man, J. Phys. **G26**, 771 (2000).

[48] G.W. Carter, O. Scavenius, I.N. Mishustin, and P.J. Ellis, Phys. Rev. C **61**, 045206 (2000).

[49] Let us remind that $N_f = N_c$.

[50] It would be more reasonable to apply this additional normalization factor to the lattice data. However, we do not want to distort the “experimental” results.